

1 Supplementary Information: Coherent optical communications using  
2 coherence-cloned Kerr soliton microcombs

3 Yong Geng<sup>1,3</sup>, Heng Zhou <sup>\*1,3</sup>, Xinjie Han<sup>1</sup>, Wenwen Cui<sup>1</sup>, Qiang Zhang<sup>1</sup>, Boyuan Liu<sup>1</sup>,  
4 Guangwei Deng<sup>2</sup>, Qiang Zhou<sup>2</sup>, and Kun Qiu<sup>1</sup>

5 <sup>1</sup>Key Lab of Optical Fiber Sensing and Communication Networks, University of Electronic  
6 Science and Technology of China, Chengdu 611731, China

7 <sup>2</sup>Institute of Fundamental and Frontier Sciences, University of Electronic Science and Technology  
8 of China, Chengdu 611731, China

9 <sup>3</sup>These authors contributed equally: Yong Geng, Heng Zhou

10 **1 Influence of fiber nonlinearity on microcomb re-generation and data**  
11 **interconnect.**

12 As mentioned in the main text, the pump laser  $C_{Tx}(0)$  and pilot tone  $C_{Tx}(17)$  of the transmitter  
13 comb propagate through the 50 km fiber link together with the high speed data signals . A  
14 matter of concern is that the data signals may impose linewidth broadening to them via cross-  
15 phase modulation (XPM) and may degrade their spectral purity as the conveyed pump laser and  
16 reference pilot [1]. Here we conduct numerical simulation to investigate how  $C_{Tx}(0)$  and  $C_{Tx}(17)$   
17 are impacted by fiber nonlinearity. The simulation contains  $20 \times 21$  GBaud single-polarization  
18 16QAM signals with a spacing of 100 GHz. The 0th and 17th frequency bins are not modulated  
19 to mimic the  $C_{Tx}(0)$  and  $C_{Tx}(17)$  . The data on each channel are uncorrelated among the other  
20 channels. The power of each data channel is set to 0 dBm, in consistency with the experimental  
21 situation. The fiber length is 50 km in our experiment without intermediate amplification.

22 Fig. S1 shows the simulation results. It is seen that when the fiber chromatic dispersion is  
23 turned off in the simulation, XPM induces sizable temporal phase drifts on the pump laser and  
24 pilot tone. In our simulation the temporal phase drifts are extracted by beating them with a

---

\*zhouheng@uestc.edu.cn

25 zero-linewidth laser tone thus converting their phase fluctuations into amplitude fluctuations. To  
 26 the contrary, when the fiber chromatic dispersion is turned on, XPM induced phase fluctuations  
 27 become much smaller. As interpreted in the main text, chromatic dispersion of the fiber induces  
 28 spatiotemporal walk-off among signals at different wavelengths (i.e., different data channels) along  
 29 the transmission link, therefore, XPM imposed to the pump laser  $C_{Tx}(0)$  and pilot tone  $C_{Tx}(17)$   
 30 from different data channels are smoothed out as a quasi-constant phase envelop without high  
 31 frequency component, which would not impact their efficacy as pump laser and pilot tone.

32 To confirm the above numerical analysis, we conduct a separate experiment where the 20 data  
 33 channels are transmitted to the receiver within a different fiber from the pump laser  $C_{Tx}(0)$  and  
 34 pilot tone  $C_{Tx}(17)$ , so that to totally eliminate the XPM interactions between data channels and  
 35 the pump/pilot tones. As shown in Fig. S1c, data receiving SNR and BER are identical regardless  
 36 of whether one fiber or two fibers are adopted, confirming that XPM causes no prominent influence  
 37 in our system.

## 38 **2 Optical phase lock loop for two-point locking of the transmitter and** 39 **receiver microcombs.**

40 The schematic of the optical phase lock loop (OPLL) for locking  $C_{Tx}(17)$  and  $C_{Rx}(17)$  is presented  
 41 in Fig.S2. The  $\sim 941.1$  MHz beat note between the  $C_{Tx}(17)$  and  $C_{Rx}(17)$  is produced using a fast  
 42 photodetector, which is then down mixed within a double-balanced mixer to zero with a 941.1 MHz  
 43 local oscillator signal from a signal synthesizer. The down mixed signal is low-pass filtered and  
 44 used as the error signal in a proportional–integral–derivative controller (PID, Newport LB1005),  
 45 which generates the control signal to actuate the amplitude modulation of the auxiliary laser for  
 46 generating and tuning  $C_{Rx}$ , with a feedback loop bandwidth of 100 kHz. The actuation response  
 47 speed of the repetition rate of  $C_{Rx}$  is considered faster than the loop bandwidth, as instantaneous  
 48 change of the pump laser detuning can be imposed by the change of intra-cavity power of the  
 49 auxiliary laser through the effect of XPM [2]. The residual phase noises from the OPLL and the  
 50 signal synthesizer are considered responsible for the imperfect phase coherence between the carrier  
 51 and LO (see Fig. 1 and Fig. 3 of the main text) after two-point locking.

## 52 **References**

- 53 [1] Abel Lorences-Riesgo, Tobias A. Eriksson, Attila Fulop, Peter A. Andrekson, and Magnus Karlsson. Frequency-comb  
54 regeneration for self-homodyne superchannels. *Journal of Lightwave Technology*, 34(8):1800–1806, 2016.
- 55 [2] George N. Ghalanos, Jonathan M. Silver, Leonardo Del Bino, Niall Moroney, Shuangyou Zhang, Michael T. M. Woodley,  
56 Andreas Ø. Svela, and Pascal Del’Haye. Kerr-nonlinearity-induced mode-splitting in optical microresonators. *Physical*  
57 *Review Letters*, 124(22):223901, 2020.

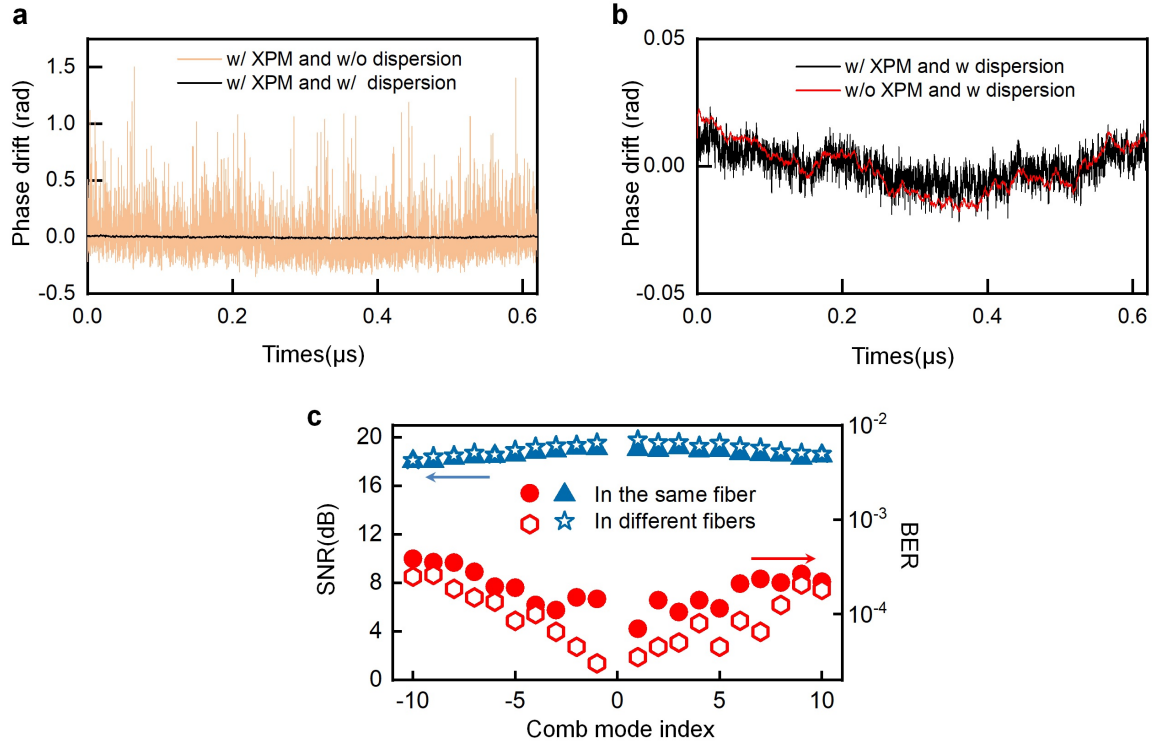


Fig. S1: **Simulation results of phase degradation induced by fiber nonlinearity.** **a.** Comparison of the phase deterioration by fiber XPM effect between the cases with and without chromatic dispersion. **b.** Comparison of phase deterioration between with and without XPM effect. **c.** Comparison of experimental measured data receiving SNR and BER when 20 data channels and the pump/pilot tones are transmitted in the same fiber or in different fibers.

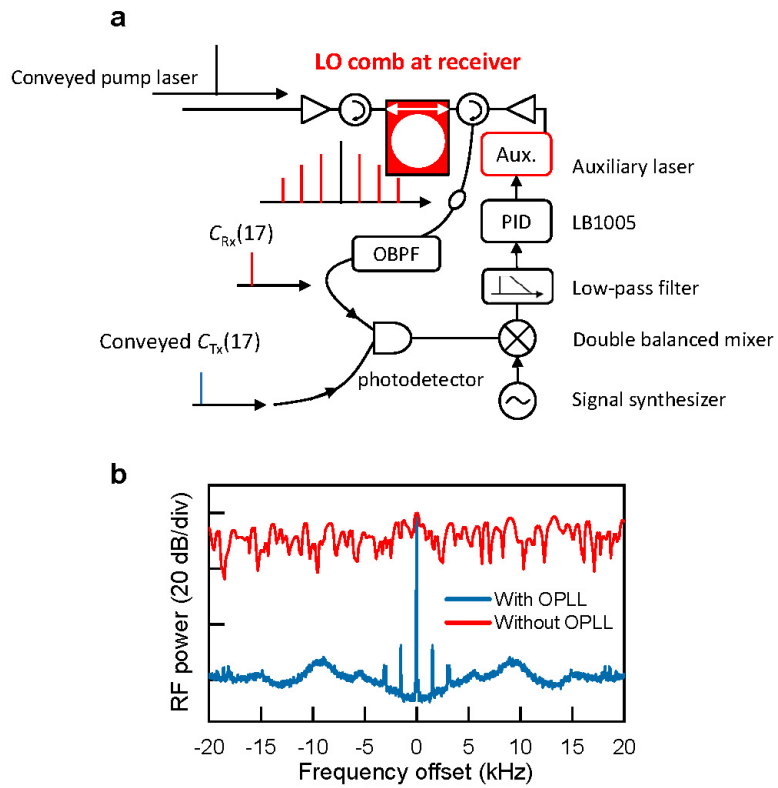


Fig. S2: **a.** Experimental setup of the OPLL for locking of  $C_{Tx}(17)$  and  $C_{Rx}(17)$ . **b.** Comparison of the beat notes between  $C_{Tx}(17)$  and  $C_{Rx}(17)$  with and without using OPLL.